

# Optical Coherence Tomography as an Auxiliary Tool for the Screening of Radiation-Related Caries

Cláudia Cristina Brainer de Oliveira Mota, DDS, MSc,<sup>1</sup> Luiz Alcino Gueiros, DDS, PhD,<sup>1</sup>  
Ana Marly Araújo Maia, DDS, MSc,<sup>1</sup> Alan Roger Santos-Silva, DDS, PhD,<sup>2</sup>  
Anderson Stevens Leonidas Gomes, PhD,<sup>3</sup> Fábio de Abreu Alves, DDS, PhD,<sup>4</sup>  
Jair Carneiro Leão, DDS, PhD,<sup>1</sup> Anderson Zanardi de Freitas, PhD,<sup>5</sup>  
Mário Goes, DDS, PhD,<sup>6</sup> and Márcio Ajudarte Lopes, DDS, PhD<sup>2</sup>

## Abstract

**Objective:** The aim of this study was to evaluate the morphological alterations of radiation-related caries using optical coherence tomography. **Methods:** Thirty-six extracted teeth from 11 patients who had undergone radiotherapy were sectioned in the sagittal axis in the center of the carious lesion, and 100  $\mu\text{m}$  thick sections were obtained from each specimen. One sample from each tooth was investigated by an optical coherence tomography (OCT) system, and the results were compared with histological images from polarized light microscopy. **Results:** In OCT dentin caries images, the demineralized area appeared as a white region, whereas the translucent zone appeared as a dark area, a similar pattern also seen in coronal caries. In noncavitated enamel lesions clinically observed as brown discoloration, the area of high porosity, and also the dark color, absorbs part of the light, resulting in a dark pattern. Finally, the involvement of dentin–enamel junction (DEJ) or cement–enamel junction (CEJ) could be clearly observed, when present and marked alterations along the CEJ could be noted, as junction continuity loss, gap formation, and mineral loss tissue. **Conclusions:** The OCT technique was able to characterize radiation-related caries, from a morphological point of view. Also demonstrated was its potential benefit for use in the clinical monitoring of radiation-related carious process.

## Introduction

PATIENTS UNDERGOING HEAD AND NECK RADIOTHERAPY often develop early and late oral complications. Of these, radiation-related caries (RRC) is the most threatening to dental structure. It is considered a unique disease because of its rapid onset and progression, with a high potential for dental destruction (amputation of crowns and complete loss of dentition within short periods of time), affecting mainly cervical areas, after exposure of the cement–enamel junction (CEJ) and/or the dentin–enamel junction (DEJ).<sup>1,2</sup> Although the exact nature of RRC has not been completely understood, it can be considered as a complex and multifactorial disease related to the direct and indirect effects of radiation on the salivary glands and teeth.<sup>3–8</sup>

Despite recent advances in radiation therapy and implementation of multidisciplinary approaches, the oral en-

vironment of patients who undergo head and neck therapy still poses a clinical challenge for dentistry. Therefore, a better understanding of carious development in patients with cancer could be useful for the improvement of clinical management.

Polarized light microscopy (PLM) is classically used to evaluate dental caries, and can be an adequate tool to evaluate RRC, as previously described.<sup>3</sup> Optical coherence tomography (OCT) is a nondestructive imaging technique using low-coherence interferometry to determine the time delay and magnitude of backscattered light reflected off a transparent and semitransparent structure.<sup>9</sup> By using the optical properties of reflection and scattering into sound and carious mineralized tissues, it is possible to evaluate and characterize morphological structures as the CEJ and DEJ.<sup>10</sup> The aim of this *ex vivo* study was to analyze the morphological properties of RRC using OCT, which has the advantage of being

<sup>1</sup>Departamento de Clínica e Odontologia Preventiva, Universidade Federal de Pernambuco, Recife-PE, Brazil.

<sup>2</sup>Departamento de Diagnóstico Oral, Universidade Estadual de Campinas – UNICAMP, Piracicaba – SP, Brazil.

<sup>3</sup>Departamento de Física, Universidade Federal de Pernambuco, Recife-PE, Brazil.

<sup>4</sup>Departamento de Estomatologia, Hospital do Câncer AC Camargo, São Paulo, SP, Brazil.

<sup>5</sup>Instituto de Pesquisas Energéticas e Nucleares, IPEN-CNEN/SP, São Paulo – SP, Brazil.

<sup>6</sup>Departamento de Odontologia, Restauradora, Universidade Estadual de Campinas–UNICAMP, Piracicaba–SP, Brazil.

noninvasive and nondestructive – therefore having potential clinical use – and to further match such results with the PLM findings.

### Materials and Methods

The study analyzed 36 human permanent teeth in different stages of the RRC process evolution, extracted because of advanced periodontal disease, from 11 patients who had received radiotherapy for head and neck cancer treatment. The clinicopathological aspects of the studied patients were previously presented by our group.<sup>3</sup> All the selected teeth were within the irradiation field, and after extraction, the teeth were stored in 10% neutral-buffered formalin solution. The analysis was conducted after approval by the Ethics Committee for Human Studies at Piracicaba Dental School, Brazil (process number 167/2006), according to the Declaration of Helsinki.

Visual inspection was performed, analyzing the external aspect of teeth surfaces, in order to detect the presence and extent of carious lesions in the samples.

### OCT experimental setup

A commercially available OCT system was used (Spectral Radar SR-OCT: OCP930SR/Thorlabs, NJ), operating in the spectral domain using a superluminescent diode (SLD) light source at central wavelength of 930 nm. This system consisted of three main parts: a handheld scanning probe, a base unit, and a personal computer (PC) (Fig. 1). The base unit contained the SLD light source. A fiberoptic coupler was used to direct the light from a broadband SLD source to the Michelson interferometer, which was located inside the handheld probe. The sample and the reference light traveled

back through the same fiber to the spectrometer and the imaging sensor located in the base unit. The base unit was connected to the PC, which was equipped with two high-performance data acquisition cards. All required data acquisition and processing were performed via the integrated software package, which included a complete set of functions for collection and control data measurement of OCT image files. The software was developed in LabVIEW (Laboratory Virtual Instrument Engineering Workbench, National Instruments, USA) language program. Images were generated as a numerical matricial array, composed in 2000 columns and 512 lines, and the maximum lateral scanning was 6.0 mm, which provided  $6.2 \mu\text{m}$  of axial and transversal resolution when combined with the optical system. The system captured approximately three frames per second, and the maximum image depth was 1.3 mm.

### Samples evaluation by OCT

OCT performs high-resolution and cross-sectional tomographic imaging of the internal structures in biological tissues by measuring the backscattered and reflected light as a function of the scattering caused by the local changes in tissue structure of the tooth, as different refractive indexes for each kind of tissue, for example enamel or dentin, presenting carious or noncarious lesion. Variations in scattering measured in relation to depth from a single point on the tooth surface are called an “A-scan”. Taking several A-scans along a line produces information from a “slice” of tooth tissue, which is the tomogram. The movement along the line of A-scans is known as the “B-scan.”<sup>11</sup>

OCT images (B-scan) were acquired perpendicular to the sample surface firmly positioned to avoid dislocations, aiming to identify the enamel and dentin caries zones,

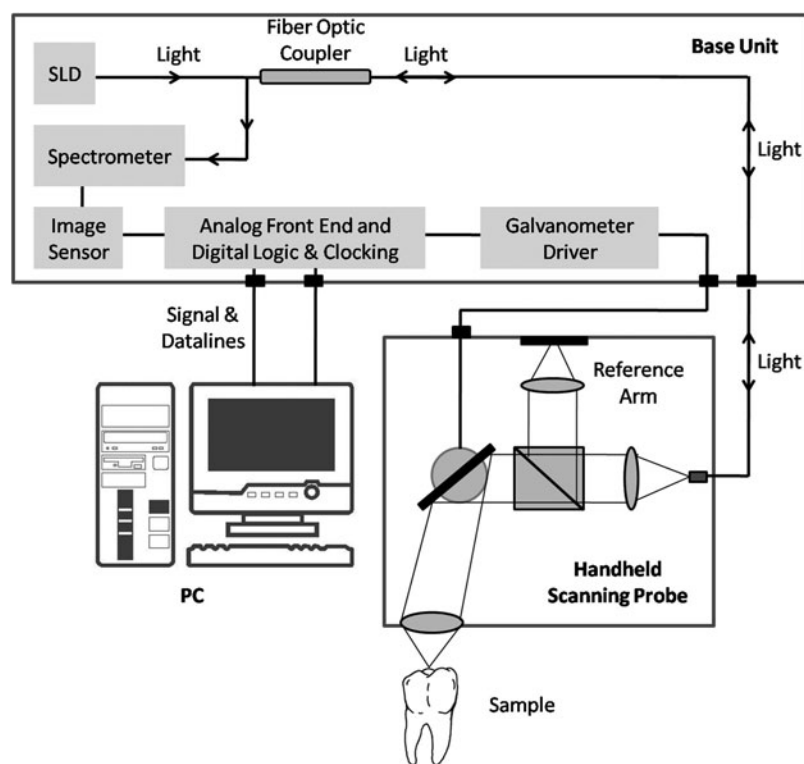


FIG. 1. The commercial SR-OCT, OCP930SR, schematic diagram (adapted from Thorlabs, NJ).

qualitative patterns of demineralization and reactionary dentin. The charge-coupled device (CCD) system attached was applied as a guide to visually observe the cross-sectional images obtained every 200  $\mu\text{m}$  longitudinally. This sequence of images sections gave a complete mapping of the internal structures. All images were scaled by LabVIEW software, and the quantitative measurements were obtained using public domain software, Image J (Imaging Processing and Analysis in Java, National Institutes of Health, Bethesda, MD). To confirm the analysis of internal structures – the transition from enamel to dentin, the limit between sound and carious tissue, or even the presence of caries affecting the CEJ and/or DEJ – A-scans of specific points as a function of depth were analyzed using the software Origin 8.1 (Origin-LAB Data Analysis and Graphing Software, Microcal Software Inc., USA).

### Microscopic analysis

Each tooth was sectioned in the sagittal axis in the center of the caries lesion, using a low-speed saw (Isomet, Buehler, Lake Bluff, IL) under constant water irrigation, and 100  $\mu\text{m}$  thick sections were obtained from each specimen. Hand-ground polishing was performed using successively finer grade silicon carbide paper to a final thickness of 80  $\mu\text{m}$ . Then samples were immersed in deionized water, between a glass slide and a cover-slip. One section from each tooth was investigated by transmitted PLM (DM 5.000; Leica, Wetzlar, Germany), through a 50 $\times$  magnification, in order to identify the enamel and dentin caries zones, qualitative patterns of demineralization and reactionary dentin. Images were captured by a CCD camera coupled to the PLM and analyzed by the Leica Qwin (Leica, Wetzlar, Germany) image capture software.

PLM images were then compared to OCT images, aiming to identify the alterations on enamel and root surfaces. Characteristic structures were observed under both techniques, as the demineralized dentin in the triangular pattern and in the half-moon-like shape in coronal lesions and incipient root surfaces, incisal caries and CEJ and DEJ alterations. It is important to register the presence of DEJ alterations even in noncavitated enamel lesions.

### Results

Incisors, molars, and canines were the predominant teeth, representing 42%, 31%, and 17%, respectively. Brown discoloration affecting enamel and root surfaces in the majority of the sample (81%) was observed. Also, cervical caries was visually diagnosed in 78% of the specimens, and 31% of the anterior teeth presented with incisal caries. For a better understanding of the results, Fig. 2 shows an OCT image section of the CEJ region registering cement, dentin, enamel, and their junctions in a sound and nonirradiated tooth (Fig. 2a), and the same structures in a decayed tooth, previously subjected to head and neck radiotherapy, where the altered DEJ, destroyed CEJ, and carious progress in both cement and dentin (Fig. 2b) can be seen. Cement is presented as a thin well-defined white layer, and both junctions (CEJ and DEJ) can be easily identified as a point between the “V” depression and a dark line below enamel, respectively.

PLM findings were used as the gold standard to compare with OCT images (Fig. 3). By PLM, the triangular pattern (Fig. 3a) and half-moon-like shape (Fig. 3b) of demineral-

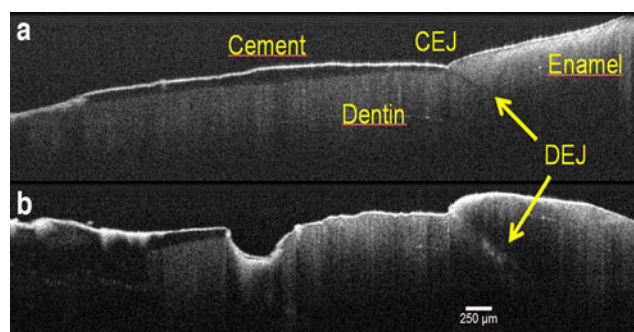


**FIG. 2.** Cross-sectional optical coherence tomography (OCT) image of sound and nonirradiated tooth (a), showing the enamel, dentin, cement, dentin-enamel and cement-enamel junctions, and an irradiated tooth (b), presenting the caries progress affecting the same structures.

ization in coronal lesions and incipient root surface caries (with the base at the tooth surface and the apex pointing to the pulp) were identified as demineralized dentin and translucent zone.

In OCT dentin caries images, the demineralization promotes an increased reflectivity and loss of light intensity on the deeper portions of the tooth.<sup>12</sup> Therefore, the demineralized area appeared as a white region because of the increase in the backscattered and reflected light associated with alteration of the refractive index and increased porosity. The translucent zone appeared as a dark area because of the lower backscattered light. A similar pattern could be observed in coronal caries and incipient surface caries (Fig. 3e and f).

Incisal caries (Fig. 3c and g), with triangular demineralization affecting the exposed dentin with little involvement of enamel by PLM, were shown in OCT images with similar aspects, sparing the enamel and involving the DEJ. OCT images of noncavitated brown-discolored enamel (Fig. 3d and h) presented as an area of high light absorption; the dark color absorbed a considerable amount of the light, diminishing its penetration. In addition, DEJ was not clearly observed because of the reduction of light penetration in the sub-superficial lesion.

Moreover, marked alterations along the cement and CEJ could be observed as loss of cement and its continuity, as well as CEJ disorganization as seen in Fig. 4a–c, which show different sections of the same tooth, evidencing the DEJ and CEJ loss of continuity, with the caries propagation through the DEJ, even under the apparently sound enamel. These findings can possibly explain the higher dentin surface exposition, the presence of gaps, and DEJ demineralization process. In Fig. 4c, it is possible to observe, on the right side, an area of dentin caries immediately after the DEJ limit; at the opposite side, there is healthy dentin under the remaining cement. The microleakage through the DEJ shown in Fig. 4d clearly represents a gap (the spreading of demineralization process) as a marked white line formed because of the presence of a thin air-occupied space between the dentin and enamel. In the sample, DEJ and/or CEJ changes were noted as a well-defined white line in 25/27 teeth (92.59%) and extensive areas of dentin exposure were noted in 22/27 teeth (81.5%).

In addition, OCT cross-sectional images allow quantification of the depth of mineral loss tissue. Figure 4e and f, from

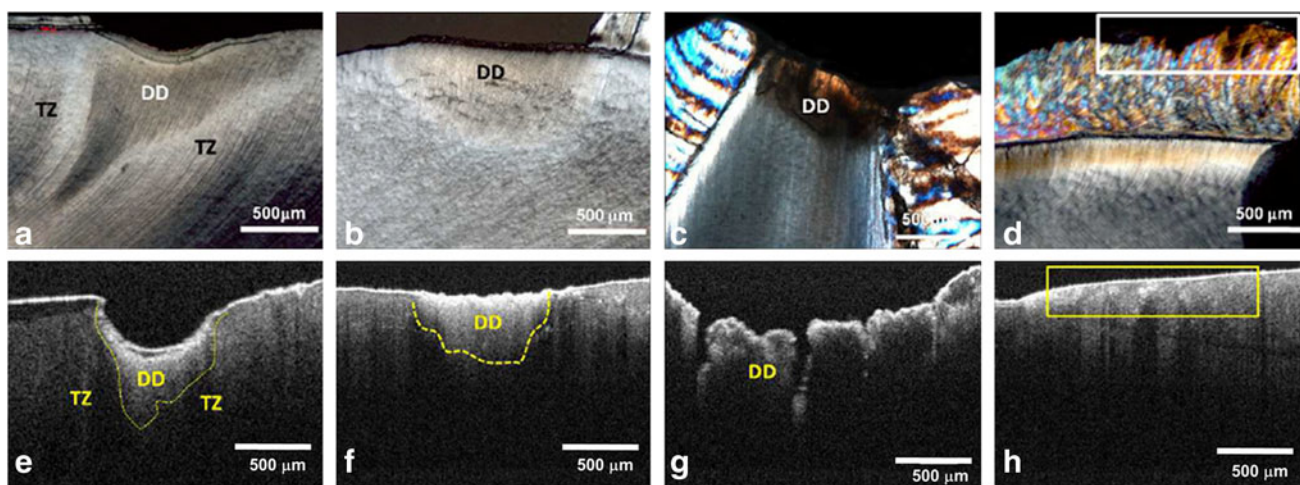


**FIG. 3.** Polarized light microscopy (PLM) micrographs of deep coronal caries lesion (a), incipient root surface caries (b), incisal caries (c), and brown discoloration in noncavitated smooth surface of enamel (into rectangle) (d). Corresponding optical coherence tomography (OCT) images, respectively (e–h). DD, demineralized dentin; TZ, translucent zone.

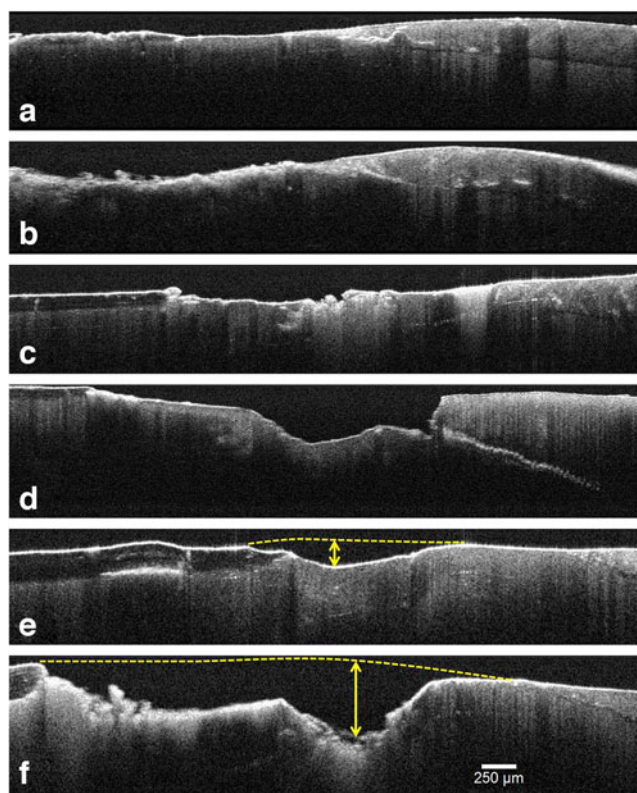


**FIG. 4.** Optical coherence tomography (OCT) images (a–c) show different sections of the same tooth. In addition to evidencing the DEJ and CEJ alterations, in (c) an area of dentin caries near to the DEJ and healthy dentin under the remaining cement is also observed. (d) Microleakage through the DEJ (gap), caused by caries and abrasion lesions. (e and f) Caries progression in different parts of the same tooth. Maximum depth was measured to evolve from 189 to 485  $\mu\text{m}$  (dashed lines are guides to the eyes).

different parts in the same tooth, show the loss of mineral tissue resulting from the caries progress, whose maximum depth was measured to evolve from 189  $\mu\text{m}$  (Fig. 4e) to 485  $\mu\text{m}$  (Fig. 4f). Differences in cement structure and its architectural organization could be easily noted. On the other hand, PLM had shown a significant birefringence and some destruction around the CEJ region. In addition, OCT analysis showed DEJ alterations through sound enamel, allowing better identification, and also measuring the depth of carious lesions even in these situations.

## Discussion

Although similar microscopic aspects among “standard” caries and RRC have been found,<sup>3</sup> additional understanding is necessary, especially regarding brown discolorations and CEJ alterations. Only a few studies have evaluated teeth extracted following radiation therapy,<sup>1,3,13–15</sup> usually through PLM and scanning electronic microscopy (SEM). To the best of our knowledge, this is the first study conducted with OCT technique to characterize RRC. OCT technology has given valuable information of clinical use of dental materials,<sup>16,17</sup> being also capable of evaluating carious teeth. The alterations in the CEJ and DEJ identified by OCT analysis seem to be the first described. Interestingly, these alterations were also observed in “regular” caries, suggesting additional similarities between both diseases.

OCT technique analyzes the reflected and backscattered light incident on the tooth, making it possible to visualize structures inside the specimen. OCT, as a relatively novel method for the assessment of caries, is being validated in several aspects of dental diagnosis. In the present study, the technique is able to describe morphologically the RRC without the need to destroy samples, as occurs in optical microscopy, because of the nondestructive property of the method. For this reason, OCT is a promising technique to analyze the carious process evolution in irradiated patients.

More importantly, OCT images can be compared with histological images, allowing accurate identification of the enamel layer, the DEJ, and a thin layer of dentin.<sup>10</sup> In

addition, it allows identification of distinctive aspects of carious lesions, mainly as an increase in backscattered intensity, and determining of the depth of demineralization.<sup>11</sup> When comparing OCT and PLM, similar findings could be noted. Predominantly, cross-sectional images of dentin caries showed formation of reactive dentin characterized as a scattering area surrounding by translucent zone as a dark area (Fig. 4e and f), similar to the report of Silva et al.<sup>3</sup> under PLM analysis.

The difference between the dark and light regions in OCT and PLM images is caused by the nature of the interaction of light with tissue. In PLM images, the region that suffered a demineralization results in disorganization of enamel prisms, and this technique uses linear polarizers to perform the measurement. Therefore, the orientation of the polarizers is chosen to provide the best contrast in images. In the OCT images, the interaction mechanism is entirely different; the light interaction with tissue is based on the backscattering properties of the sample. With dental tissue loss mineral content there is an increase in backscattering coefficient, possibly related to the distinctive interfaces' appearance in a light propagation medium (higher porosity). These interfaces result in variations of the refractive index material, thereby changing the backscatter. Therefore, the greater the backscattered light, the lighter the OCT images will be, as it is based on backscattered signal intensity.

Clinically, RRC affects smooth surfaces, including mandibular anterior teeth, which is unexpected, as these areas are the most caries-resistant areas in nonirradiated subjects. Subsequently, there are changes in translucency and color, leading to increased friability and breakdown of the tooth.<sup>2</sup> Also, areas of enamel demineralization were frequently observed by Silva et al.<sup>3</sup> under PLM, and also confirmed by OCT analysis, being characterized as diffuse and infiltrative brown spots that clinically corresponded to those widely spread brown discolorations in the smooth surface of non-cavitated enamel. These lesions are macroscopically described as diffuse brown discoloration, and should be considered a characteristic sign of RRC.<sup>3,13</sup>

The CEJ analysis showed interesting results. Increasing age and continuous passive eruption compensating for wear at the incisal and occlusal surfaces along with gingival recession may promote a shift of the CEJ to the gingival sulcus, characterizing an area at high risk for pathological changes such as dentin sensitivity; root surface caries; and cervical erosion, resorption, and abrasion.<sup>18</sup> The dentin exposure at the CEJ added to reduced salivary flow and inadequate oral hygiene may favor a fast-growing carious process. OCT images of RRC lesions showed initial CEJ instability even when no clinical signs were observed (Fig. 4a and b). Even carious lesions associated with abrasion on the cervical region behaved as a critical point of destruction through the CEJ, affecting the DEJ as well (Fig. 4d).<sup>19</sup>

On the other hand, the DEJ is an interface between two mineralized tissues with different compositions and biomechanical properties, which can also be altered in unique conditions such as an irradiated mouth. DEJ is also believed to play an important role in preventing crack propagation from enamel to dentin, and inhibiting further tooth fracture.<sup>20,21</sup> The few publications<sup>22,23</sup> describing morphological changes in the DEJ showed gap formation where massive colonization of bacteria is often found. Adding xerostomia and poor oral hygiene may promote fast-growing enamel destruction.

Physical properties of the DEJ (e.g., width, microhardness, and elastic modulus) may provide critical information about the "crack-prevention" function.<sup>5,6,22</sup> Understanding if it can be directly altered following radiation therapy is yet a matter of debate.<sup>22</sup> A recent *in vitro* study showed a reduced ultimate tensile strength when tested perpendicularly to tubule orientation of coronal and radicular irradiated dentine, demonstrating that irradiation can be directly harmful to organic dental components.<sup>24</sup>

## Conclusions

In the present study, it was demonstrated that OCT showed some important advantages when compared with the microscopy method to evaluate RRC, the main one being the fact that it is noninvasive and can be used in the clinic. The structural changes of the cervical region, including mineral loss tissue and CEJ and DEJ alterations were also better evaluated using OCT than with PLM. As OCT provides real time 2D or 3D reconstruction images, it can be used for the screening of RRC, particularly in brownish non-cavitated areas of the teeth.

## Acknowledgments

The authors acknowledge the National Council for Scientific and Technological Development (CNPq), Brazil, for supporting this research (process: 474697/2012-6). The authors also thank Mario Fernando de Goes (Dental Materials Area) and Marcelo Giannini (Restorative Dentistry Area) from Piracicaba Dental School, University of Campinas, Brazil, for their support and contribution with sample preparation and polarized light microscopy analysis.

## Author Disclosure Statement

No competing financial interests exist.

## References

1. Vissink, A., Jansma, J., Spijkervet, F.K., Burlage, F.R., and Coppes, R.P. (2003). Oral sequelae of head and neck radiotherapy. *Crit. Rev. Oral. Biol. Med.* 14, 199-212.
2. Kielbassa, A.M., Hinkelbein, W., Hellwig, E., and Meyer-Lückel, H. (2006). Radiation-related damage to dentition. *Lancet Oncol.* 7, 326-335.
3. Silva, A.R.S., Alves, F.A., Antunes, A., Goes, M.F., and Lopes, M.A. (2009). Patterns of demineralization and dentin reactions in radiation-related caries. *Caries Res.* 43, 43-49.
4. Kielbassa, A.M., Beetz, I., Schendera, A., and Hellwig, E. (1997). Irradiation effects on microhardness of fluoridated and non-fluoridated bovine dentin. *Eur. J. Oral Sci.* 105, 444-447.
5. Grötz, K.A., Duschner, H., Kutzner, J., Thelen, M., and Wagner, W. (1997). New evidence for the etiology of so-called radiation caries. Proof for directed radiogenic damage of the enamel-dentin junction. *Strahlenther Onkol.* 173, 668-676.
6. Al-Nawas, B., Grötz, K.A., Rose, E., Duschner, H., Kann, P., and Wagner, W. (2000). Using ultrasound transmission velocity to analyse the mechanical properties of teeth after *in vitro*, *in situ*, and *in vivo* irradiation. *Clin. Oral Invest.* 4, 168-172.

7. Ail, Y., Mobasser, A.E., Warnke, P.H., Terheyden, H., Wiltfang, J., and Springer, I. (2005). Detection of mature collagen in human dental enamel. *Calcif. Tissue Int.* 76, 121–126.
8. Springer, I.N., Niehoff, P., Warnke, P.H., Bock, G., Koyacs, G., Suhr, M., Wiltfang, J., and Ail, Y. (2005). Radiation caries-radiogenic destruction of dental collagen. *Oral Oncol.* 41, 723–728.
9. Huynh, G.D., Darling, C.L., and Fried, D. (2004). Changes in the optical properties of dental enamel at 1310 nm after demineralization. *Proc. SPIE* 5313, 118–124.
10. Maia, A.M., Fonseca, D.D., Kyotoku, B.B.C., and Gomes, A.S.L. (2010). Characterization of enamel in primary teeth by optical coherence tomography for assessment of dental caries. *Int. J. Paediatr. Dent.* 20, 158–164.
11. Hall, A., and Girkin, J.M. (2004). A review of potential new diagnostic modalities for caries lesions. *J. Dent. Res.* 83, C89–C94.
12. Louie, T., Lee, C., Hsu, D., Hirasuna, K., Manesh, S., Staninec, M., Darling, C.L., and Fried, D. (2010). Clinical assessment of early tooth demineralization using polarization sensitive optical coherence tomography. *Lasers Surg. Med.* 42, 738–745.
13. Silva, A.R.S., Alves, F.A., Berger, S.B., Giannini, M., Goes, M.F., and Lopes, M.A. (2010). Radiation-related caries and early restoration failure in head and neck cancer patients. A polarized light microscopy and scanning electron microscopy study. *Supp. Care Cancer.* 18, 83–87.
14. Jongebloed, W.L., Gravenmade, E.J., and Retief, D.H. (1988). Radiation caries. A review and SEM study. *Am. J. Dent.* 1, 139–146.
15. Jansma, J., Vissink, A., Jongebloed, W.L., Retief, D.H., and Gravenmade, E. (1993). Natural and induced radiation caries: A SEM study. *Am. J. Dent.* 6, 130–136.
16. Braz, A.K.S., Kyotoku, B.B.C., Braz, R., and Gomes, A.S.L. (2009). Evaluation of crack propagation in dental composites by optical coherence tomography. *Dent. Mater.* 25, 74–79.
17. Matheus, T.C.U., Kauffman, C.F.M., Braz, A.K.S., Mota, C.C.B.O., and Gomes, A.S.L. (2010). Fracture process characterization of fiber-reinforced dental composites evaluated by optical coherence tomography, SEM and optical microscopy. *Braz. Dent. J.* 21, 420–427.
18. Arambawatta, K., Peiris, R., and Nanayakkara, D. (2009). Morphology of the cemento-enamel junction in premolar teeth. *J. Oral Sci.* 51, 623–627.
19. Schroeder, H.E., and Scherle, W.F. (1988). Cementoenamel junction – revisited. *J. Periodontal Res.* 23, 53–59.
20. Kielbassa, A.M., Hellwig, E., and Meyer-Lueckel, E. (2006). Effects of irradiation on in situ remineralization of human and bovine enamel demineralized in vitro. *Caries Res.* 40, 130–135.
21. Xu, C., Yao, X., Walker, M.P., and Wang, Y. (2009). Chemical/molecular structure of the dentin–enamel junction is dependent on the intratooth location. *Calcif. Tis. Int.* 84, 221–228.
22. Pioch, T., Golfels, D., and Staehle, H.J. (1992). An experimental study of the stability of irradiated teeth in the region of the dentinoenamel junction. *End. Dent. Traumatol.* 8, 241–244.
23. Raab, W., Petsghelt, A., and Voss, A. (2009). Rastreelektronenmikroskopische unter suchungen zur radiogenen Karies. *Strahlenther Onkol.* 45, 425–427.
24. Soares, C.J., Castro, C.G., Neiva, N.A., Soares, P.V., Santos-Filho, P.C.F., Naves, L.Z. et al (2010). Effect of Gamma Irradiation on Ultimate Tensile Strength of Enamel and Dentin. *J. Dent. Res.* 89, 159–164.

Address correspondence to:

Luiz Alcino Gueiros

Departamento de Clínica e Odontologia Preventiva – UFPE

Av. Prof. Moraes Rego, 1235

Recife-PE

Brazil

E-mail: luiz.mgueiros@ufpe.br